Journal of Structural Geology, Vol. 13, No. 3, pp. 329 to 335, 1991
Printed in Great Britain

0191-8141/91 $03.00+0.00

Strain analysis method using the maximum frequency of unimodal deformed orientation distributions: applications to gneissic rocks

JUAN IGNACIO SOTO

Instituto Andaluz Geología Mediterránea and Dpto., Geodinámica, CSIC-Univ. de Granada, 18071- Granada, Spain

(*Received* 22 *February* 1990; *accepted in revised form* 27 *July* 1990)

Abstract—The effect of varying strain ratio (R_a) on initially uniform and non-uniform orientation distributions of passive marker lines is calculated. The frequency graphs for uniform distributions have a unimodal form (*Gaussian-like distribution*), centered in the finite extension direction (X) of the strain ellipse. The maximum frequency is related to the strain. Using non-uniform distributions the frequency graph has a different unimodal pattern. The difference between the measured strain ratio (R) with the maximum frequency and the true strain ratio (R_a) to the initial distribution is quantified for different types of distribution.

The method is applied to samples of gneiss from southern Spain, using the orientation of tourmaline and feldspar lying in the schistosity plane, with respect to the stretching lineation. The strain of the marker distribution has been quantified, and after distinguishing the initial type of distribution, the true strain ratio of the whole rock in the schistosity plane can be estimated.

INTRODUCTION

STRAIN analysis using linear or planar distributions of passive markers was developed initially by March (1932) for strain-modified homogeneous distributions. Subsequently, Owens (1973) extended March's theory to any initial type of distribution. Sanderson (1973, 1977), Roberts & Sanderson (1974), Harvey & Laxton (1980), De Paor (1981) and Sanderson & Meneilly (1981) have used orientation distributions of lines with passive behaviour, in deformed rock, to determine the two- and three-dimensional strain. They showed that the shape of the strain-modified frequency distribution is related to both the amount of strain and the initial type of distribution. Alternatively, the length of linear markers has been used also by Panozzo (1984, 1987), Sanderson & Phillips (1987) and Wheeler (1989).

Deformed distribution analysis can be performed using the shape of frequency graphs (Lloyd 1983) with the asymmetry (β_1, coefficient of skewness) and the peakness (β_2, coefficient of kurtosis) parameters, or using a vectorial approach, through the calculation of the magnitude and the orientation of the resultant addition vector (r) (Mardia 1972, Sanderson 1977).

The aim of this work is to present a strain analysis method in two dimensions using the maximum frequency of the unimodal distributions of passive marker lines. The theoretical basis for this analysis was first developed by Sanderson (1977). To find the initial type of distributions the maximum frequencies observed and the expected values of known theoretical distributions are compared.

STRAIN-MODIFIED UNIFORM DISTRIBUTION

Sanderson (1977) studied the effect of non-rotational (coaxial) deformation on an initially uniform orientation distribution of passive linear markers. He showed that the initial distribution has a constant frequency (F) in a grouping interval or interval width W:

$$F_{\Delta\alpha_i} = \frac{NW}{S} \quad \begin{matrix}(0 < W \leq S) \\ (S = 180°,\ S = 360°).\end{matrix} \qquad (1)$$

After the deformation, the expected frequency in an interval (α_1', α_2') is:

$$F_{\Delta\alpha_i} = \frac{N}{S}[\tan^{-1}(R_a \tan\alpha_2') - \tan^{-1}(R_a \tan\alpha_1')], \qquad (2)$$

where α_i and α_i' are the angles of any line measured with respect to the orientation of the extension axis (X) of the finite strain ellipse, before and after the deformation, respectively (Fig. 1). R_a is the finite ratio of the strain ellipse or true strain ratio ($R_a = (1 + e_1)/(1 + e_2)$) and N is the number of lines studied (sample size).

The strain-modified uniform distribution plotted in a frequency graph (F vs α_i' or α_i), has a symmetric and unimodal shape, with the maximum frequency at $\alpha_i' = 0$ (X direction). Sanderson (1977) and Fernandez (1978, 1987) showed that the frequency distribution follows an elliptical law, where relative frequency is related to the square of the strain ratio R_a, in any direction. The comparison between this distribution and a Gaussian frequency distribution (see Sanderson 1977, fig. 3) shows a close similarity in the maximum frequency area. For this reason strain-modified uniform distributions will be treated as a *Gaussian-like distribution*, specified by:

$$F_{\Delta\alpha_i'} = \frac{N}{\sigma\sqrt{2\pi}} \exp\left[\frac{(\mu - \alpha_i')}{\sigma\sqrt{2}}\right]^2,$$

where μ is the arithmetic mean of the frequency distribution and σ is the standard deviation.

The linear markers rotate, with the deformation, towards the extension direction of the finite strain ellipse

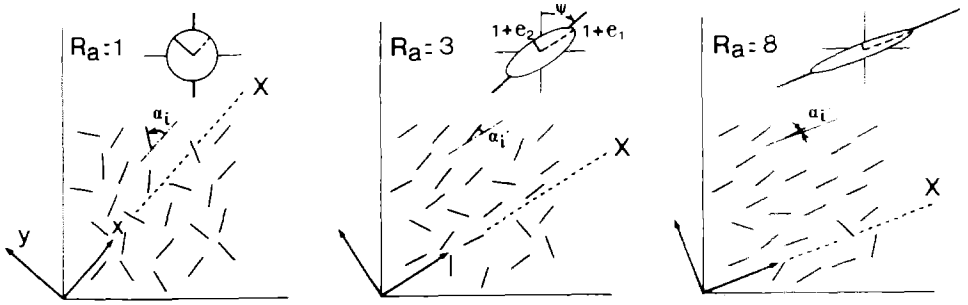

Fig. 1. Rotation of passive linear markers during progressive simple shear deformation. Finite strain ellipse rotates towards the 'horizontal' axis of the reference system as a function of the angular shear strain, ψ. The ellipticity of the finite strain ellipse is R_a, and is equal to $(1 + e_1)/(1 + e_2)$ (short axis with continuous line and long axis with broken line). The marker orientation around the finite extension direction as the strain rate increases is showed by the progressive decrease in α_i' value.

(X) (Fig. 1). The number of elements near the X-axis orientation, expressed by the maximum frequency in a frequency graph, increases with increasing deformation (Fig. 2a). It is important that the axis of the reference system coincide with the finite principal strain axis (Fig. 1). There is no difference, with this orientation criterion, between rotational and non-rotational deformations (cf. Lloyd 1983, Fernandez 1987) and the frequency distributions have the mean value centred at $\alpha_i' = 0$. The interval (α_1', α_2'), centred on the origin, has a maximum frequency (F_m). If α_1' and α_2' have small values the expression (2) can be simplified:

$$F_m = \frac{N}{S} R_a(\alpha_2' - \alpha_1');$$

$$R_a = \frac{SF_m}{N(\alpha_2' - \alpha_1')}. \quad (3)$$

In the next section it is explained how to obtain the strain ratio of a deformed distribution from the maximum frequency value (F_m) of unimodal frequency distribution using the expression (3). The measured strain ratio R is not equal to the true strain ratio R_a.

STRAIN ANALYSIS USING f_m VALUES

Linear distributions ($S = 180°$) have been used in the orientation description (α_i' and α_i) of each linear element, although the use of circular distributions and circular statistics ($S = 360°$) would be more rigorous. The angular variation rank plotted on the frequency graph is $-90° < \alpha_i, \alpha_i' \leq +90°$. When α_i or α_i' are greater than $+90°$, they are reconverted to $\alpha_i' = \alpha_i' - 180°$ (Lloyd 1983).

The effect of deformation with $2 \leq R_a \leq 20$ has been calculated using theoretical uniform initial distributions, with different sample sizes ranging from 25 to 360. The new angular value for each linear element of the strain-modified distribution is obtained applying the Wettstein equation (Ramsay 1967):

$$\tan \alpha_i' = \tan \alpha_i (R_a)^{-1}$$

to the elements of the undeformed distribution.

The distributions, deformed and non-deformed, are plotted in a frequency graph using different interval width (W) values. To normalize the frequency distribution with respect to the sample size studied (N) relative frequencies ($f = F/N$) have been used.

The graphical solution of expression (3) is plotted in a f_m vs R graph for a determined W value of 4° (Fig. 3). For R values lower than 10 the f_m values change as a function of $f_m \approx (2 \log R)/10$.

Confidence intervals for X-*axis and* R

Assuming a *Gaussian-like distribution* for the strain-modified frequency distribution it is possible to estimate confidence intervals for the X-axis position. Binomial probability tables (in Fisher 1948 and Cheeney 1983) of

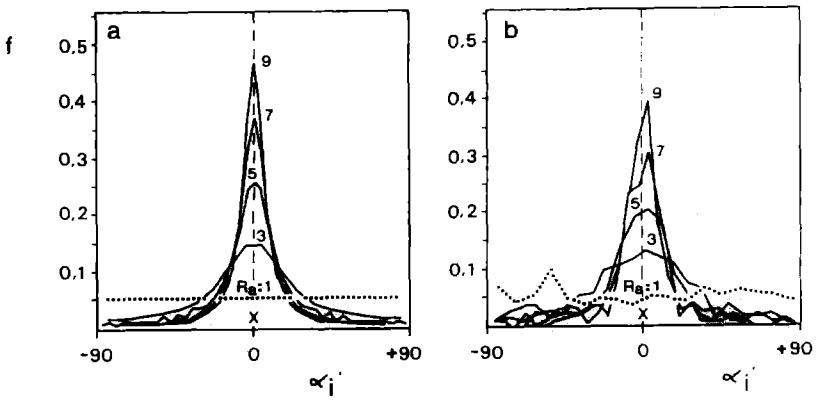

Fig. 2. Frequency graphs, f vs α_i', of: (a) strain-modified uniform distribution; (b) strain-modified non-uniform orientation distribution. Sample size of 360 elements, interval width of 10° and *modal grouping*.

the Student's test (t values) for the 95% confidence intervals have been used to estimate the X-axis position for several sample sizes. The 95% confidence interval for the orientation of the X principal strain direction in a strain-modified uniform distribution is obtained using the expression:

$$X = \mu \pm \frac{t\sigma}{N} \text{ degrees.}$$

The R values for the 95% confidence interval boundaries are calculated using the expression (3) with the X-axis 95% confidence interval. These values are plotted as broken lines in Fig. 3.

Type of grouping and population size

Fisher (1989) showed that the shape of a frequency distribution diagram is related to the interval width (W) and interval boundaries used. It has been compared for the f_m and R values obtained for different W values (e.g. $W = 4°$) and interval boundaries. Strain-modified uniform distributions are grouped with two types of interval boundaries. One, defined with respect to the mode value (α'_m) (e.g. ... $\alpha'_m - 2°/\alpha'_m + 2°$, $\alpha'_m + 2°/\alpha'_m + 6°$, ...) is called *modal grouping*, and the other with interval boundaries defined with respect to any other value (e.g. 0°, ... 0°/4°, 4°/8°, 8°/12° ...) is called *random grouping* (Figs. 4a & b, respectively). If a *random grouping* is used with continuous interval boundaries (e.g. ... 0°/4°, 1°/5°, 2°/6°, ...), the results are similar to that obtained with the *modal grouping*.

The R value obtained from strain-modified distributions grouped with different interval widths (W) decreases as W values increase. This pattern is, however, dependent on the type of grouping used (Figs. 4a & b). With *modal grouping*, R values decrease more regularly than with *random grouping*. The angle of this plot (δ angle), measured anticlockwise from a vertical line, is defined by the R values obtained with the extreme interval widths used (Rw_i) and the difference between both W ($W_1 = 2°$ or 4° and $W_2 = 10°$):

$$\delta = \tan^{-1}\left[\frac{(Rw_1 - Rw_2^*)}{(W_2 - W_1)}\right]. \quad (4)$$

The asterisk expresses the use of *modal grouping*. The δ angle value is related to the true strain ratio R_a as shown in Fig. 5.

The R value measured by this method is always less than the true strain ratio R_a. For interval widths of 2° and 4° the difference between R and R_a, ($D = R - R_a$), is smaller. The D value is minimal up to $R = 10$ ($R_a \approx R + (R \tan 3°)$) increasing exponentially for greater strain ratios. Figure 6 can be used to quantify this difference.

Sample sizes smaller than 50 measurements are not advisable for this method, because the measured R has a large variation with respect to R_a, ($R_a = R \pm 2$). The strain ratio obtained using sample sizes greater than 200 does not give more than a 3% improvement in accuracy with respect to the $N = 100$ value (Figs. 4a & b).

Non-uniform distributions

For strain measurement with angular data, the initial type of distribution considered was either uniform (Sanderson 1977, Sanderson & Meneilly 1981) or Gaussian (Sanderson 1973, Roberts & Sanderson 1974, Lloyd 1983). None of these authors have discussed strain measurement using non-uniform distributions. These types of distributions have several clusters but no single preferred orientation.

The random distribution showed in Fig. 7, with several cluster zones and without a marked orientation fabric, has been used to test the strain method in non-uniform distributions. The effect of deformation with

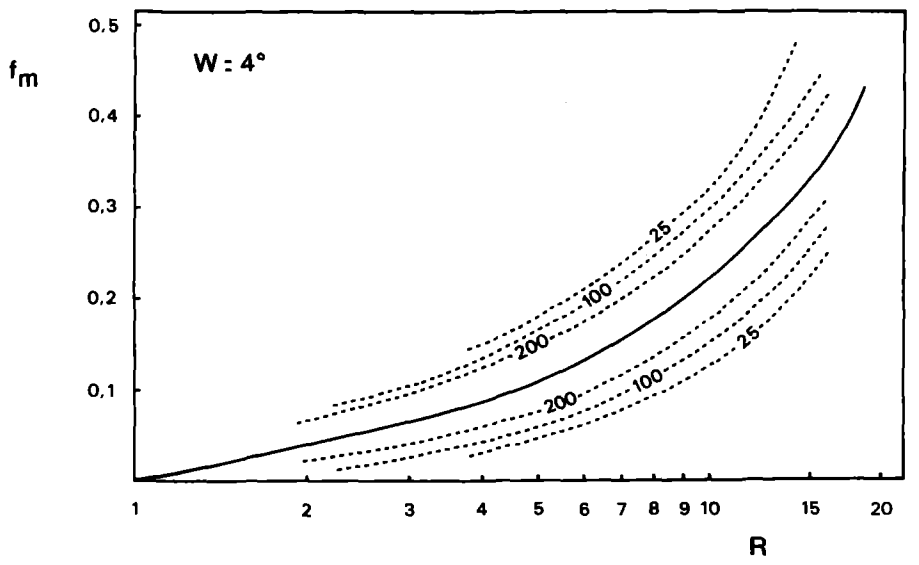

Fig. 3. Relationship between maximum relative frequency, f_m, and measured strain ratio, R, in logarithmic scale, for strain-modified uniform distributions. The discontinuous lines show the 95% confidence intervals of R, for sample sizes of 25, 100 and 200.

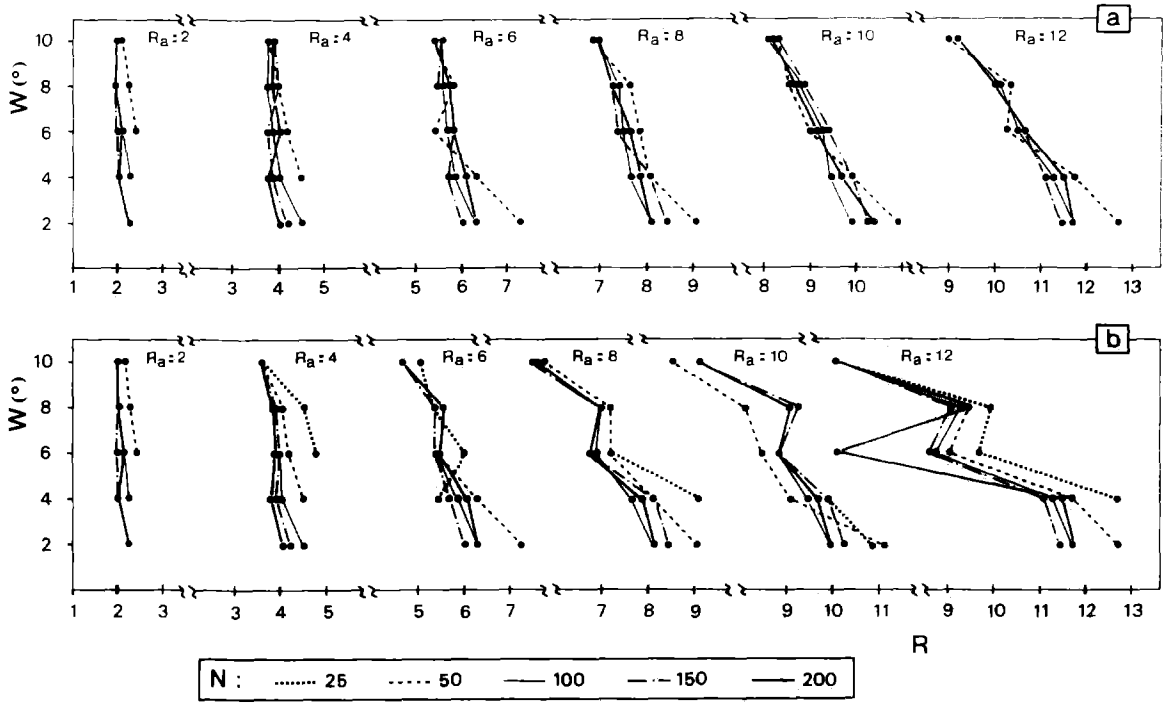

Fig. 4. Graph of interval width (W) vs measured strain ratio (R) for strain-modified uniform distributions, deformed by homogeneous strain with different values of strain ratios R_a and sample sizes, N. Type of grouping: (a) *modal grouping*; (b) *random grouping*. The angle, measured anticlockwise, between this plot from a vertical line is the δ angle.

$2 \leq R_a \leq 20$ in this distribution are compared with the results of the uniform distributions (Figs. 2a and 4). The resultant frequency graph (Fig. 2b) is unimodal with a marked asymmetric pattern. As strain rate increases the frequency graph becomes more pointed, symmetric and centred in the finite extension direction. The measured R values are always smaller than those obtained from the strain-deformed uniform distributions. For the type of non-uniform distribution used, the difference D ($D = R - R_a$) decreases linearly with the deformation, $R_a = R + (R \tan \theta)$. For this example θ = 22–25° (Fig. 6).

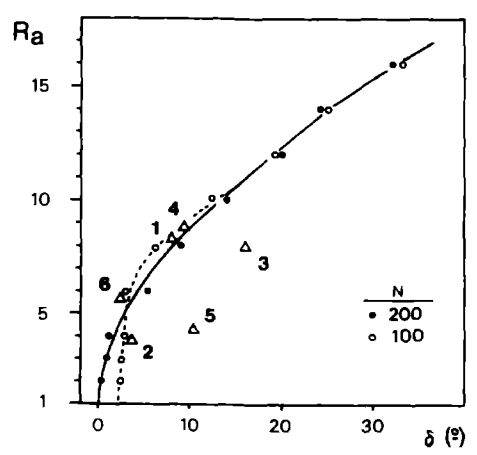

Fig. 5. Relationship between the strain ratio R_a and the δ angle for strain-modified uniform distributions. The continuous line is for sample size of 200 (close circles); the broken line for N = 100 (open circles). The numbers (1–6) and triangles refer to the six examples studied.

APPLICATION OF THE METHOD TO GNEISSIC ROCKS

The method has been applied to six outcrops in an orthogneiss body in SE Spain. These gneisses belong to the Nevado–Filabride Complex of the Betic chain (for a more detailed geological setting see García-Dueñas *et al.* 1988). The strain in several outcrops was studied by Borradaile (1976) using a de-straining method.

The examples studied have a pronounced schistosity and stretching lineation with a mean trend N100°E plunging 15–20° E. The X direction of the finite strain ellipsoid is assumed to be parallel to the stretching lineation on the schistosity plane (assumed to be the XY plane), with a 10° oscillation. This is defined by the orientation of prismatic minerals: tourmaline and feldspar, and also by quartz elongation in recrystallized ribbons. The linear markers used were ⟨c⟩ axis of tourmaline crystals and (010) traces of feldspar crystals in the XY planes. The angles between the linear markers and the X direction were measured from photographs.

The frequency distributions of the samples are plotted in Fig. 8 and the statistical parameters calculated are given in Table 1. For all the samples the mode (α'_m) and the mean (μ) of the distributions are included in the oscillation rank of the X direction ($X \pm 10°$). The values of the β_1 coefficient, which represents the asymmetry of the distributions (Lloyd 1983), are almost zero with the exception of sample 1. Both of the abovementioned observations suggest initial types of distribution without preferential orientation, and the method explained above can be applied to obtain the strain ratio in these examples.

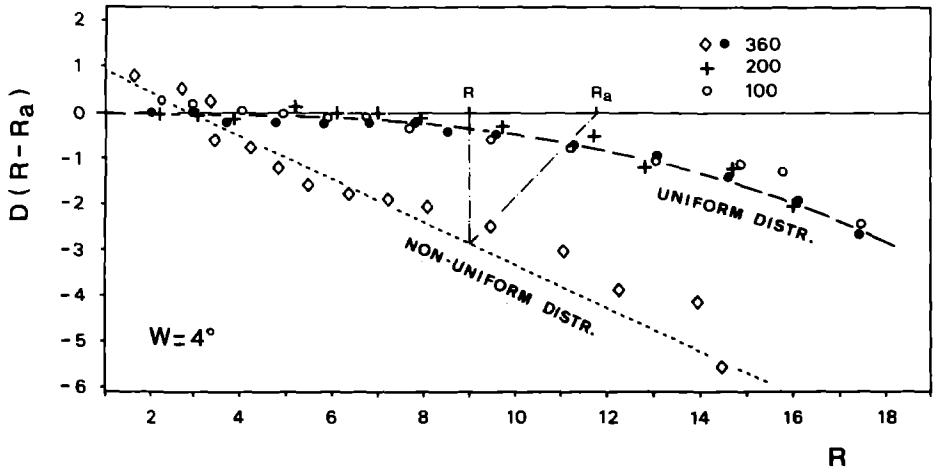

Fig. 6. Difference D ($D = R - R_a$) between the R and R_a values for strain-modified uniform distributions (heavy broken line) and strain-modified non-uniform distributions (fine broken line). Sample size is represented by solid circles (uniform distribution) and diamonds (non-uniform distribution) for 360 elements; crosses for 200 elements and open circles for 100 elements with uniform distributions. In all the cases the measured strain ratio, R, is obtained using an interval width of 4° and a *modal grouping*.

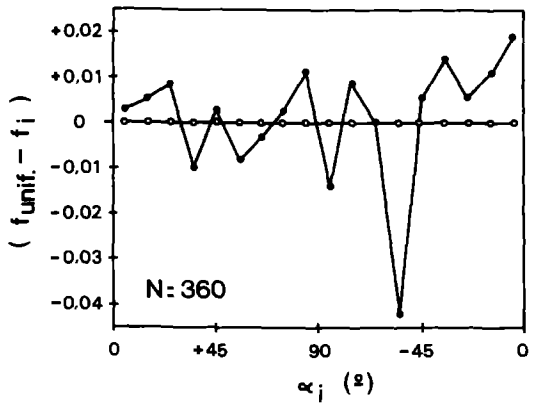

Fig. 7. Difference between the relative frequencies of the uniform distribution (open circles) and the non-uniform distribution used in the text (solid circles).

Using the f_m values in conjunction with Fig. 3, R can be measured (Table 2). The initial type of distribution can be determined using the R values for each interval width (cf. Fig. 9). The most asymmetric graphs, samples 3 and 5 ($\beta_1 > 0.2$), have R vs W variation patterns which differ from those obtained from an initially uniform distribution (cf. Figs. 9 and 4a). The initial distribution for these examples is therefore probably non-uniform and without a single preferred orientation. The other samples, 2, 4 and 6, have more symmetrical frequency distributions and also smaller β_1 values, which indicates more uniform initial distributions of crystals (Figs. 5 and 9). The anomalous β_1 parameter for the first sample can be explained by the high f_m value in α'_m at a certain distance (5.36°) from the X-axis mean position (1.36°).

Once the initial type of distribution for each sample has been estimated, the true deformation (R_a) can be obtained using Fig. 6. For the distributions closest to the uniform type, the D value is not greater than −0.5; but in distributions such as initial non-uniform types, D can achieve a value of −2 (Table 2).

DISCUSSION

Mechanical behaviour

Strain methods usually assume that during the deformation, which is homogeneous at the scale studied, the markers have a passive mechanical behaviour (March 1932, Ramsay & Huber 1983). Active markers in coaxial and non-coaxial deformations have been used also by several authors in two-dimensional (e.g. Lisle 1977, Le Theoff 1979) and three-dimensional systems (e.g. Reed & Tryggvason 1974, Shimamoto & Ikeda 1976, Blanchard *et al.* 1979, Ferguson 1979, Freeman 1985, 1987). The minerals used as markers in this rock have a non-ideal mechanical behaviour. Ghosh & Ramberg (1976), Passchier (1987) and Hanmer (1990) showed that ellipti-

Table 1. Statistical parameters of the examples studied. (Grid references are expressed in UTM co-ordinates. The asterisk (*) means *modal grouping*.) Column terms as defined in the text

Sample	Grid reference	Mineral	N	W	f_m	α'_m	δ	μ	σ	β_1	β_2
1	30SWG855164	Tourmaline	196	4	0.174	−4	8.53	1.36	21.27	1.517	6.688
2	30SWG824148	Tourmaline	159	6*	0.119	+6	3.81	12.88	28.88	0.126	4.182
3	30SWG836171	Feldspar	127	4	0.157	0	15.82	−8.15	16.88	0.402	3.884
4	30SWG822161	Feldspar	109	4	0.183	+8	9.46	6.13	10.82	0.027	4.678
5	30SWG834164	Feldspar	115	8*	0.183	−2	10.38	−10.72	34.61	0.254	3.379
6	30SWG853134	Tourmaline	129	4	0.124	−2	2.86	−3.01	17.63	0.007	5.071

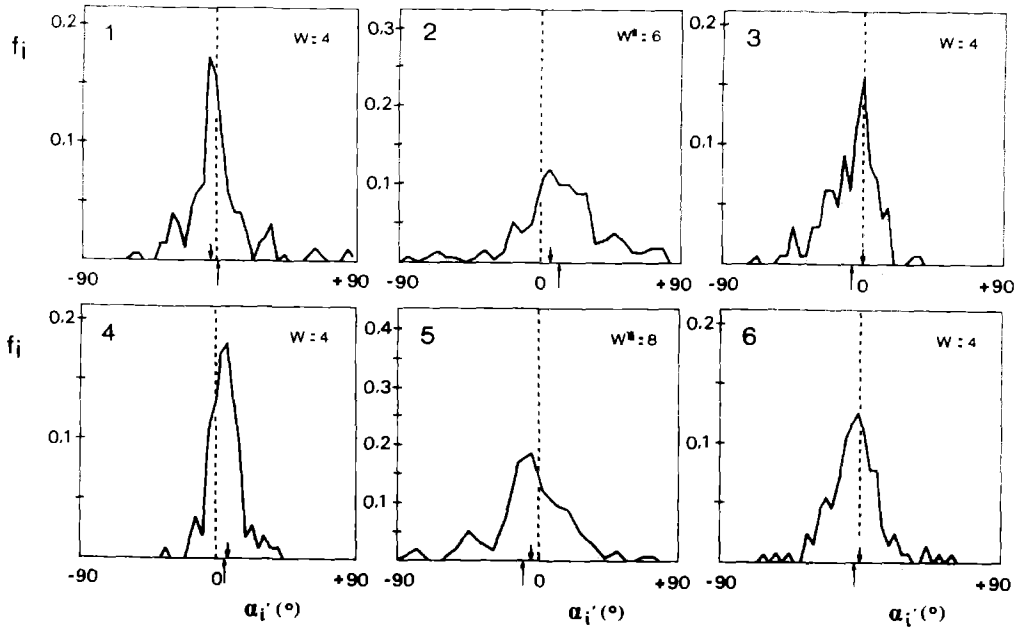

Fig. 8. Frequency graphs of the examples studied. The upwards arrow indicates the arithmetic mean (μ) and the downward arrow the mode (α'_m) of the distribution. The asterisk expresses the use of *modal grouping*. Markers used: feldspar crystals (examples 3, 4 and 5) and tourmaline acicular crystals (examples 1, 2 and 6).

cal, rigid inclusions with axial ratio greater than 10, in a viscous matrix, have a passive behaviour and rotate at the same speed as the matrix. The tourmaline crystals have elongated prismatic shapes, with axial ratios (large axis/short axis) greater than 15. The behaviour of these crystals is similar to that of rigid inclusions. There is a difference in the viscosity ratio between crystals and matrix, which is expressed as broken crystals along basal planes (110). Crystal fragmentation constitutes an important limitation to the strain analysis method, although the use of crystal fragments has been avoided. Because these crystals are preferentially broken when they reach the extension field of the strain ellipse, it produces exceptionally high values in the peakness of the frequency distribution, for example sample 1 (β_2 = 6.688).

The different microstructures of feldspar crystals indicate a relative viscosity difference between them and the matrix. This difference has a minimum expressed by pinch-and-swell effect in crystals, and a maximum expressed by σ-type porphyroclasts (Passchier & Simpson 1986). The axial ratios of the feldspar crystals are usually less than 10. Therefore these crystals rotated non-passively at a slightly lower rate than the matrix. Asymmetric frequency distributions such as found in samples 3 and 5 (β_1 = 0.25–0.4) can be explained by differences in the behaviour of the feldspar crystals and the matrix.

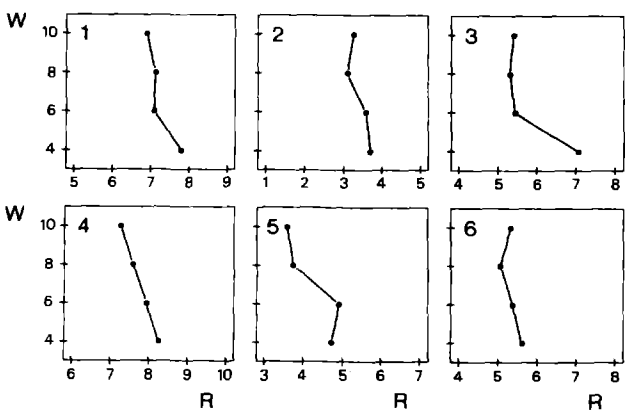

Fig. 9. Graph of interval width (W) vs strain ratio (R) for the examples studied (examples 1–6).

Type of deformation

Sanderson's (1977) original method did not consider the effects of different types of deformations. Beach (1979), using non-passive markers (belemnites), related the rotational or non-coaxial deformations to the different positions of the arithmetic mean (μ) and the mode (α'_i) in a frequency graph. Lloyd (1983) showed that the shape of the frequency plot is related to the initial type of distribution and not to the type of deformation.

The use of a reference grid coincident with the finite principal strain axis, removes the difference between non-rotational and rotational deformations. With this criterion, and strictly passive markers, the frequency distributions are always symmetrical with respect to the X-axis direction (Figs. 1 and 2) (Lloyd 1983, Fernandez 1987).

Table 2. Strain estimation of the examples studied. Column terms as defined in the text

Sample	f_m	R	95%—R	Distribution	R_a
1	0.173	7.83	5.75/10	≈ Uniform	8.2
2	0.119	3.57	2.2 / 5.75	≈ Uniform	3.7
3	0.157	7.06	5 /10	Non-uniform	7.4–8.6
4	0.183	8.24	5.75/11.7	≈ Uniform	8.7
5	0.183	4.12	3.1 / 7.6	Non-uniform	4.3–4.7
6	0.124	5.58	8.6 / 4.1	≈ Uniform	5.9

The whole rock deformation in the examples analysed is rotational. This is shown as a systematic sense of vorticity in the porphyroclast systems and in asymmetric patterns of quartz fabrics (García-Dueñas *et al.* 1988). Four of the samples (2, 4, 5 and 6) have frequency distributions with a fairly symmetrical shape ($\beta_1 < 0.27$). In the more asymmetric patterns (samples 1 and 3) the α'_m and μ values are contained in the observed variation of the X direction. The frequency distribution shape is therefore related to the strain ratio and not with the type of deformation. It is more influenced by the initial type of non-uniform distribution and the mechanical behaviour of the markers.

CONCLUSIONS

(1) This paper describes a method of strain analysis using the maximum frequency of deformed orientation distributions.

(2) Grouping the angular distributions with respect to the mode (α'_m) with different interval widths gives an estimate of the initial type of distribution, by comparison with the various patterns of strain-modified uniform distributions.

(3) The strain ratio obtained (R) is dependent on the initial type of distribution.

(4) The study of f_m values in natural frequency distributions of gneissic rocks using tourmaline and feldspar crystals lying in schistosity planes, makes it possible to determine the strain and estimate the initial distribution type. Elliptical markers must have aspect ratios larger than 10 to have a strictly passive behaviour.

(5) Asymmetric frequency distributions with respect to the orientation of the finite principal extension axis are caused by a difference in the mechanical behaviour between the markers and the matrix, and also by the initial distribution not being strictly uniform.

Acknowledgements—I am grateful to Dr J. P. Platt for his comments and critical review of a first version of this paper. Also I should like to express my gratitude to R. F. Cheeney, S. H. Treagus and an anonymous referee for their careful reviews of the text. The work was supported by the CICYT project PB 87-0461-01 and a grant from the University of Granada.

REFERENCES

Beach, A. 1979. The analysis of deformed belemnites. *J. Struct. Geol.* **1**, 127–135.

Beach, A. 1982. Strain analysis in a cover thrust zone, external French Alps. In: *Strain Within Thrust Belts* (edited by Williams, G. D.). *Tectonophysics* **88**, 333–346.

Blanchard, J.-Ph., Boyer, P. & Gagny, C. 1979. Un nouveau critère de sens de mise en place dans une caisse filonienne: le "pincement" des minéraux aux épontes (orientation des minéraux dans un magma en écoulement). *Tectonophysics* **53**, 1–25.

Borradaile, G. J. 1976. A strain study of a granite-granite gneiss transition and accompanying schistosity formation in the Betic orogenic zone, SE. Spain. *J. geol. Soc. Lond.* **132**, 417–428.

Cheeney, R. F. 1983. *Statistical Methods in Geology for Field and Lab Decisions*. George Allen & Unwin, London.

De Paor, D. G. 1981. Strain analysis using deformed line distributions. *Tectonophysics* **73**, 9–14.

Ferguson, C. C. 1979. Rotations of elongate rigid particles in slow non-Newtonian flows. *Tectonophysics* **60**, 247–262.

Fernandez, A. 1978. Fonction de distribution de l'orientation de marqueurs linéaires lors de la déformation par aplatissement à deux dimensions. *C.r. Acad. Sci. Paris* **286**, 1857–1860.

Fernandez, A. 1987. Preferred orientation developed by rigid markers in two-dimensional simple shear strain: a theoretical and experimental study. *Tectonophysics* **136**, 151–158.

Fisher, N. I. 1989. Smoothing a sample of circular data. *J. Struct. Geol.* **11**, 775–778.

Fisher, R. A. 1948. *Statistical Methods for Research Workers* (10th edn). Oliver & Boyd, Edinburgh.

Freeman, B. 1985. The motion of rigid ellipsoidal particles in slow flows. *Tectonophysics* **113**, 163–183.

Freeman, B. 1987. The behaviour of deformable ellipsoidal particles in three-dimensional slow flows: implications for geological strain analysis. *Tectonophysics* **132**, 297–309.

García-Dueñas, V., Martínez-Martínez, J. M., Orozco, M. & Soto, J. I. 1988. Plis-nappes, cisaillements syn- à post-métamorphiques et cisaillements ductiles-fragiles en distension dans les Nevado-Filabrides (Cordillères bétiques, Espagne). *C.r. Acad. Sci. Paris* **307**, 1389–1395.

Ghosh, S. K. & Ramberg, H. 1976. Reorientation of inclusions by combinations of pure shear and simple shear. *Tectonophysics* **34**, 1–70.

Hanmer, S. 1990. Natural rotated inclusions in non-ideal shear. *Tectonophysics* **176**, 245–255.

Harvey, P. K. & Laxton, R. R. 1980. The estimation of finite strain from the orientation distribution of passively deformed linear markers: eigen value relationships. *Tectonophysics* **70**, 285–307.

Le Theoff, B. 1979. Non-coaxial deformation of elliptical particles. *Tectonophysics* **53**, 7–13.

Lisle, L. 1977. Estimation of the tectonic strain ratio from the shape of deformed elliptical markers. *Geol. Mijnb.* **56**, 140–144.

Lloyd, G. E. 1983. Strain analysis using the shape of expected and observed continuous frequency distributions. *J. Struct. Geol.* **5**, 225–231.

March, A. 1932. Mathematische Theorie der Regelung nach der Korngestalt bei affiner Deformation. *Z. Kristallogr.* **81**, 285–297.

Mardia, K. V. 1972. *Statistics of Directional Data*. Academic Press, London.

Owens, W. H. 1973. Strain modification of angular density distributions. *Tectonophysics* **16**, 249–261.

Panozzo, R. 1984. Two-dimensional strain from the orientation of lines in a plane. *J. Struct. Geol.* **6**, 215–221.

Panozzo, R. 1987. Two-dimensional strain determination by the inverse SURFOR wheel. *J. Struct. Geol.* **9**, 115–119.

Passchier, C. W. 1987. Stable positions of rigid objects in non-coaxial flow—a study in vorticity analysis. *J. Struct. Geol.* **9**, 679–690.

Passchier, C. W. & Simpson, C. 1986. Porphyroclast systems as kinematic indicators. *J. Struct. Geol.* **8**, 831–843.

Ramsay, J. G. 1967. *Folding and Fracturing of Rocks*. McGraw-Hill, New York.

Ramsay, J. G. & Huber, M. I. 1983. *The Techniques of Modern Structural Geology, Volume I: Strain Analysis*. Academic Press, London.

Reed, L. J. & Tryggvason, E. 1974. Preferred orientations of rigid particles in a viscous matrix deformed by pure shear and simple shear. *Tectonophysics* **24**, 85–98.

Roberts, J. L. & Sanderson, D. J. 1974. Oblique fold axes in the Dalradian rocks of the Southwest Highlands. *Scott. J. Geol.* **9**, 281–296.

Sanderson, D. J. 1973. The development of fold axes oblique to the regional trend. *Tectonophysics* **16**, 55–70.

Sanderson, D. J. 1977. The analysis of finite strain using lines with an initial random orientation. *Tectonophysics* **43**, 199–211.

Sanderson, D. J. & Meneilly, A. W. 1981. Analysis of three-dimensional strain modified uniform distributions: andalusite fabrics from a granite aureole. *J. Struct. Geol.* **3**, 109–116.

Sanderson, D. J. & Phillips, S. J. L. 1987. Strain analysis using length-weighting of deformed random line elements. *J. Struct. Geol.* **9**, 511–514.

Shimamoto, T. & Ikeda, Y. 1976. A simple algebraic method for strain estimation from deformed ellipsoidal objects. 1. Basic theory. *Tectonophysics* **36**, 315–337.

Wheeler, J. 1989. A concise algebraic method for assessing strain in distributions of linear objects. *J. Struct. Geol.* **11**, 1007–1010.